Electronic Supplementary Material (ESI) for New Journal of Chemistry.

Anthracene based Microporous Metal-Organic Framework for Adsorbing CO_2 and Detecting TNP Sensitivity

Qingbo An, Siqi Bao*, Xiao Li*, Jing Sun and Zhongmin Su*

School of Chemical and Environmental Engineering, Changchun University of Science and Technology, Jilin Provincial Science and Technology Innovation Centre of Optical Materials and Chemistry, Changchun, People's Republic of China.

E-mail: lix@cust.edu.cn, zmsu@nenu.edu.cn.

Experimental section

Materials and measurement

All reagents and solvents for the syntheses were purchased from commercial sources and used without further purification. The ligand of 9,10-bis(1H-imidazol-1-yl)anthracene (dia) and 4,4′,4″-[1,3,5-benzenetriyltris(carbonylimino)]tris(benzoate) (H_3L) were synthesized according to the reported literature[1,2]. Infrared spectra were obtained from KBr pellets in a wavelength ranging from 4000-400 cm^{-1} on a Nicolet 380 FT-IR spectrophotometer. The C, H, and N elemental analyses were measured using a PerkinElmer 240 CHN elemental analyzer. Photo-luminescence spectra were measured using a F-4600 FL spectrophotometer equipped with a xenon lamp and a quartzcarrier at ambient temperature. Powder X-Ray diffraction (PXRD) patterns were acquired on a Siemens D5005 automated diffractometer with Cu Ka (l = 1.5418 Å) radiation in the range of 5-50°. Thermogravimetric analysis (TGA) was conducted on a Perkin-Elmer FLS-920 analyzer heated from ambient temperature to 800 ℃ under argon atmosphere at a ramp rate of 5 ℃ min^{-1}.

X-ray Crystallographic Analysis

A Bruker SMART APEX II CCD diffractometer with a graphite monochromator was used to record the X-ray single crystal diffraction data of CUST-607 under the conditions of MoKα radiation (λ = 0.71073Å) at 298 K. A multiscan technique was applied to perform adsorption corrections. The structure was solved using the direct method and refined using the full matrix least-square techniques on F^2 with anisotropic

thermal parameters for all non-hydrogen atoms using the SHELXL-97 program. All hydrogen atoms are refined isotropically, and they are all located in the calculated position. In 1, the disordered atoms C4 and C106, and C37 and C105, N6 and N16, N11 and N17 were disordered over two sites with occupancy of 0.5 and were anisotropically refined. The crystallographic data for CUST-607 has been deposited in the Cambridge Crystallographic Data Centre with the deposition number CCDC 2166871. The crystal data and structure refinement results of CUST-607 is summarized in Table S1 (ESI†).

Synthesis and Methods

A mixture containing $Cd(NO)_3 \cdot 4H_2O$ (30 mg, 0.1 mmol), dia (30 mg, 0.1 mmol), and H_3L (16 mg, 0.1 mmol) was dissolved in 8 mL of DMA-EtOH-H_2O (1:1:2, v/v), and then the solutions was stirred for 30 min at ambient temperature. Then the mixture was placed in a 23 mL Teflon-lined autoclave under autogenous pressure and heated at 100 °C for 3 days. After cool to ambient temperature, quite a few light-yellow blocks of crystals were obtained, washed with methanol, and dried under ambient conditions. Yield: 51 mg (51% yield based on dia). Anal. Calcd for $C_{104}H_{79}Cd_3N_{15}O_{22}$: C, 56.01; H, 3.54; N, 9.42. Found: C, 55.28; H, 3.87; N, 8.99. IR (KBr, cm^{-1}): 3453 m, 3126 m, 1671 m, 1497 m, 1402 w, 1150 m, 1022 m, 920 m, 762 m, 650 m, 588 m, 433 m.

The infrared spectrum is mainly composed of carboxyl group, benzene ring and anthracene ligand (Figure S5). The peaks at 3453 and 3126 cm^{-1} belong to the stretching vibration of O-H bond, the peaks at 1400-1600 cm^{-2} are the infrared characteristic peaks of benzene ring, and the peaks at 600-950 cm^{-2} correspond to anthracene ligand.

Photoluminescence Experiments

The finely ground sample (3 mg) was immersed in 2 mL corresponding solution, treated by ultrasonication for 30 min, and subsequently aged to make the suspension stable enough for measurement.

Detection of explosives

Dissolve the analyte in DMF and prepare it into a solution with different concentrations. Then take 1 mL of the solution and add it into the sample tube containing 1 mg of crystal powder. After ultrasonic treatment for 30 min, disperse it evenly and form a stable suspension. Let it stand for 1 min. Test it by fluorescence spectrometer to check

the quenching condition of the material. Check the selective quenching of different analytes according to the quenching condition of the material.

Computational details

The fluorescence quenching was analyzed using the Stern-Volmer equations [3]:

$$I_0/I = 1 + K_{SV}[M]$$

where I_0 and I are the fluorescence intensity, in the absence and presence of analyte, respectively, K_{SV} is the Stern-Volmer quenching constant and [M] is the concentration of analyte.

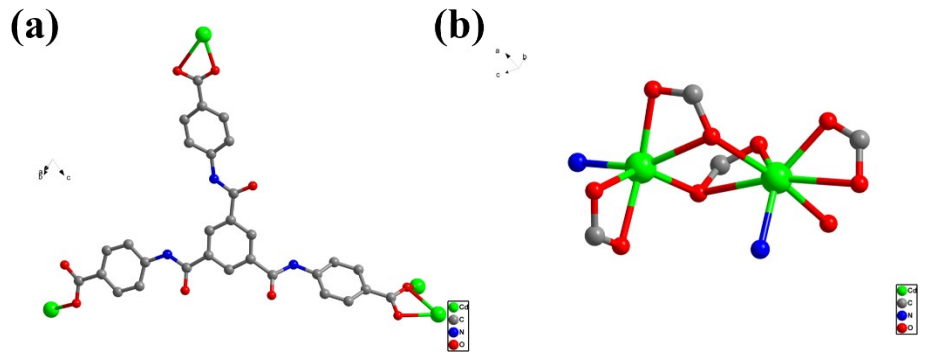

Figure S1 (a) The coordination modes of H_3L; (b) Binuclear Chromium Cluster in CUST-607.

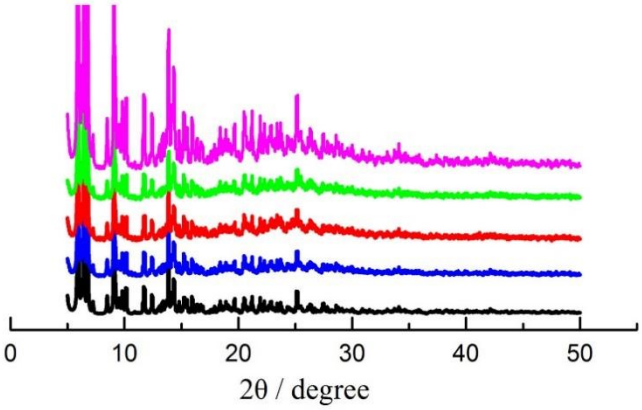

Figure S2. Experimental (blue), simulated (black), the NB experimental (red), the TNP experimental (green) and the gas adsorption (purple) PXRD patterns for CUST-607.

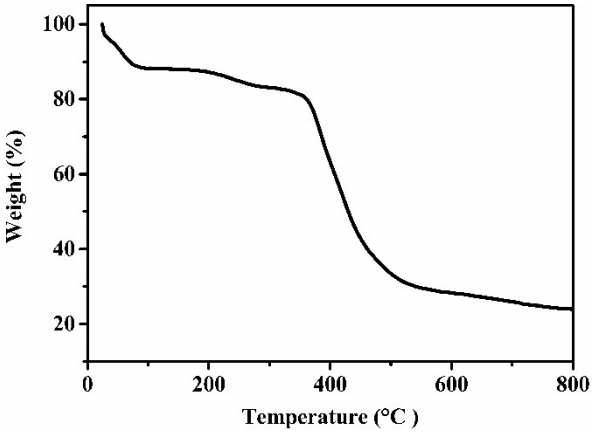

Figure S3. The TGA curve for CUST-607.

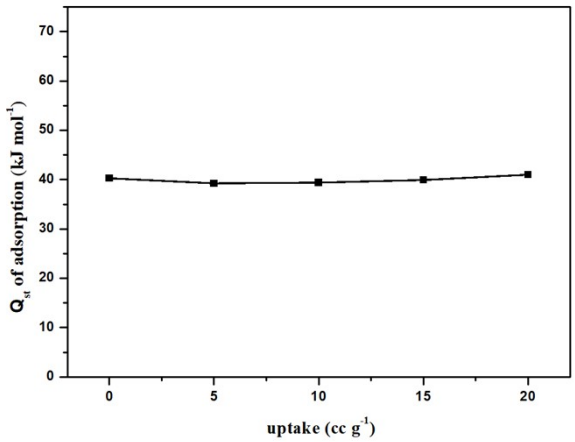

Figure S4. The isosteric heat of adsorption (Q_{st}) of CO_2 for CUST-607.

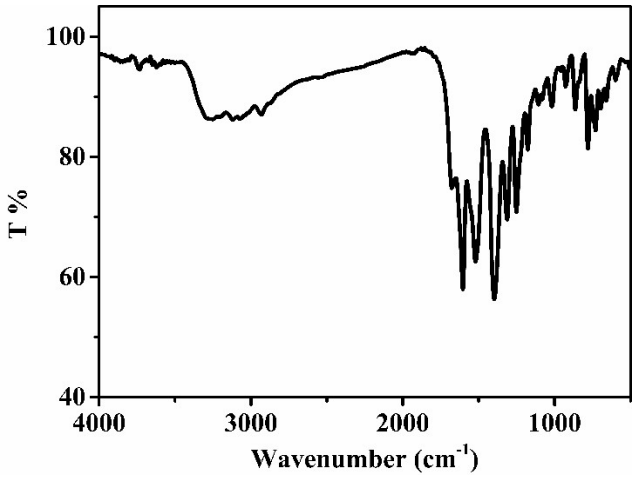

Figure S5. FTIR spectrum of CUST-607.

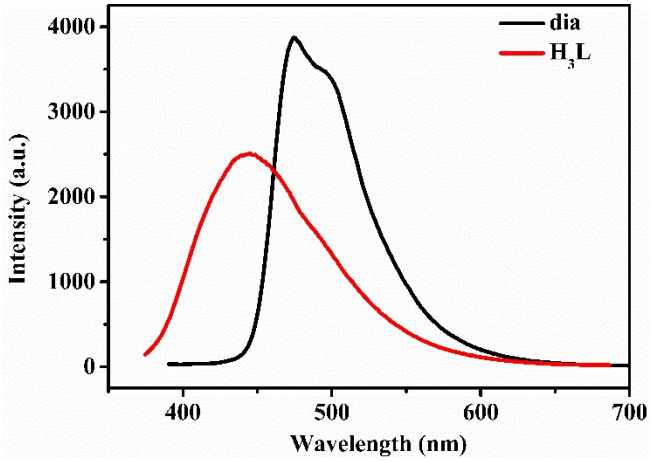

Figure S6. Emission spectra of ligands.

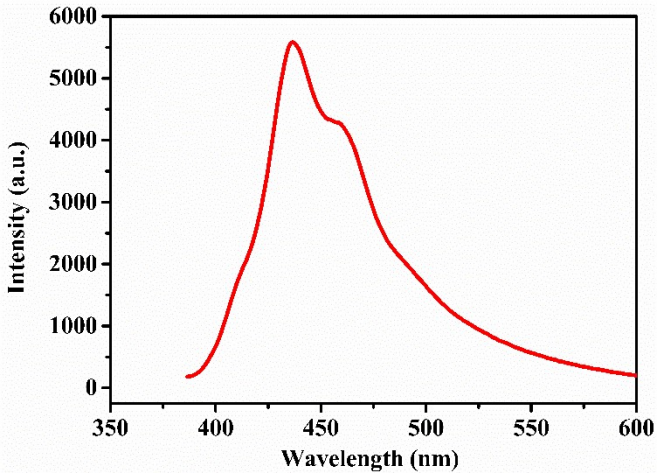

Figure S7. Emission spectra of CUST-607.

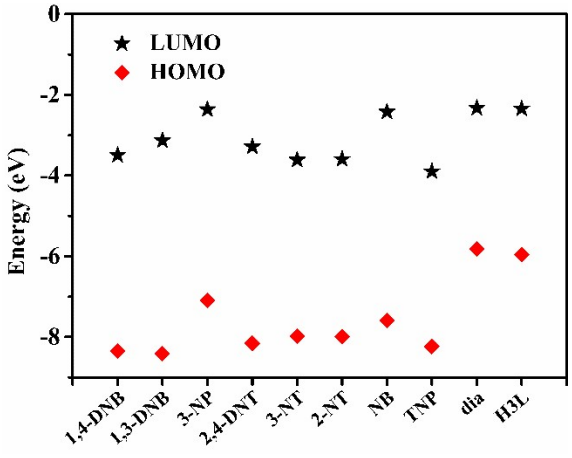

Figure S8. Theoretical LUMO and HOMO energies levels of nitro explosives and ligands.

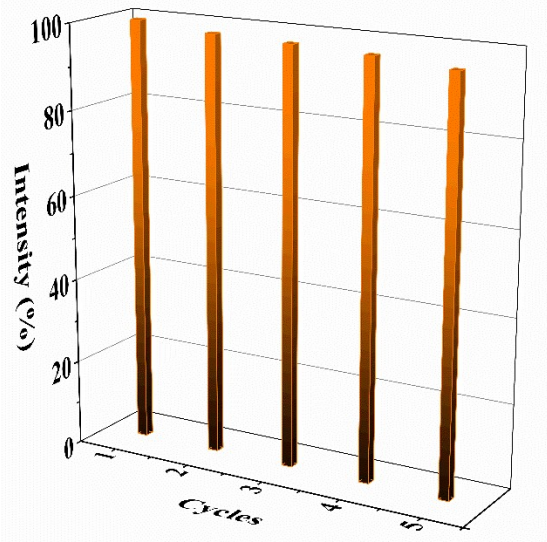

Figure S9. The quenching and recyclability test of CUST-607.

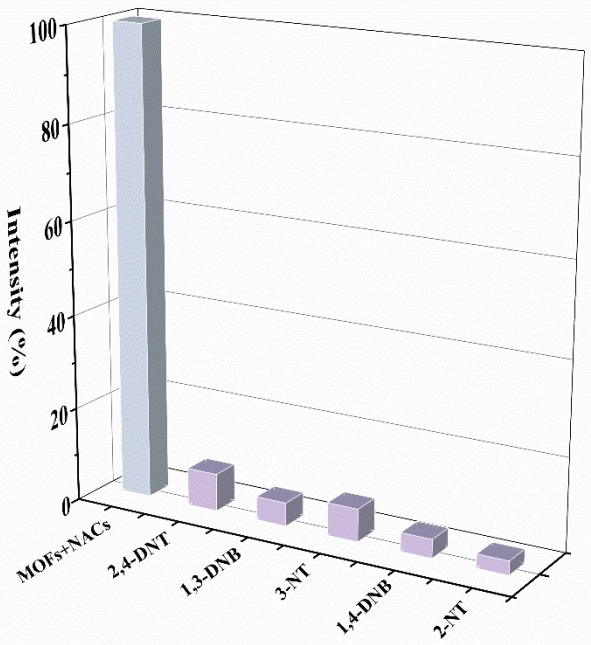

Figure S10. The anti-interference experiments of CUST-607 for detecting TNP.

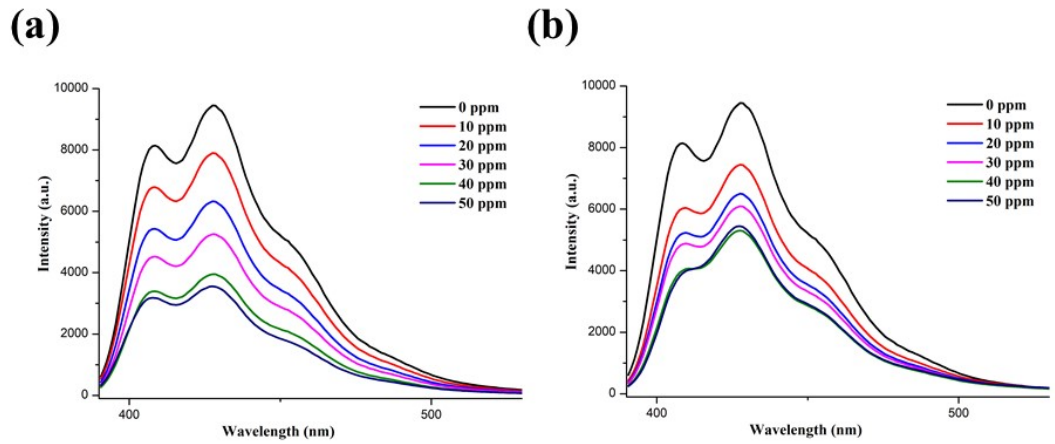

Figure S11. Fluorescence titration experiments in the range of 0-50 ppm; (a)3-NP; (b) 2-NT.

Table S1 Crystallographic data and structure refinements for CUST-607.

	$[Cd_3(H_2O)(H3L)_2(dia)_2]\cdot 4DMA\cdot 10H_2O$
Empirical formula	C116H122Cd3N18O33
Formula weight	2633.51
Temperature/K	296.15
Crystal system	triclinic
Space group	P-1
a/Å	16.4608(9)
b/Å	19.5414(11)
c/Å	21.2468(12)
α/°	73.8090(10)
β/°	68.6360(10)
γ/°	73.2410(10)
Volume/Å^3	5977.6(6)
Z	2
Goodness-of-fit on F^2	0.925
Final R indexes [I>=2σ (I)]	R_1 = 0.0495 wR_2 = 0.1067
Final R indexes [all data]	R_1 = 0.0911 wR_2 = 0.1165
ρ_{cal}cg/cm^3	1.463
μ/mm^{-1}	0.595
F (000)	2256.0
Radiation	Mo Kα (λ = 0.71073)

Index ranges	$-19 \leq h \leq 17$ $-23 \leq k \leq 13$
	$-25 \leq l \leq 25$
Reflections collected	34574
Independent reflections	21043[R_{int} = 0.0389 R_{sigma} = 0.0842]
Data/restraints/parameters	21043/82/1333
2Θ range for data collection/°	3.128 to 50
Largest diff. peak/hole / e Å^{-3}	0.62/-0.81

Table S2 Selected bond lengths [Å] and Selected angles [˚] for CUST-607.

Bond	**Distance (Å)**	**Bond**	**Distance (Å)**
Cd(1)-O(8)	2.166(3)	Cd(1)-N(1)	2.221(4)
Cd(1)-O(11)#1	2.171(3)	Cd(1)-N(3)	2.278(4)
Cd(2)-O(2)	2.246(4)	Cd(2)-N(14) #3	2.246(4)
Cd(2)-O(3)	2.470(3)	Cd(3)-N(4)	2.194(4)
Cd(2)-O(4)	2.265(3)	Cd(3)-O(13) #4	2.235(4)
Cd(2)-O(9) #2	2.312(3)	Cd(3)-O(16)	2.178(3)
Cd(2)-O(10) #2	2.347(4)	Cd(3)-O1W	2.466(5)
Cd(3)-O(3) #4	2.389(3)		
[1]+X,-1+Y,+Z; [2]+X,1+Y,+Z; [3]2-X,2-Y,-Z; [4]+X,+Y,-1+Z; [5]1-X,-Y,4-Z; [6]-X,-Y,4-Z			
Bond	**Angle (°)**	**Bond**	**Angle (°)**
O(8)-Cd(1)-N(1)	130.52(13)	O(10) #2-Cd(2)-O(3)	98.62(12)
O(8)-Cd(1)-N(3)	99.07(14)	N(1)-Cd(1)-N(3)	95.24(13)
O(8)-Cd(1)-O(11)#1	100.10(14)	N(14)#3-Cd(2)-O(3)	154.76(13)
O(11)#1-Cd(1)-N(1)	109.31(15)	N(14)#3-Cd(2)-O(4)	101.56(14)
O(11)#1-Cd(1)-N(3)	125.37(14)	N(14)#3-Cd(2)-O(9)#2	91.41(14)
O(2)-Cd(2)-O(3)	80.66(11)	N(14)#3-Cd(2)-O(10)#2	94.43(14)
O(2)-Cd(2)-O(4)	109.83(12)	O(3)#4-Cd(3)-O1W	165.29(14)
O(2)-Cd(2)-O(9)#2	90.43(13)	N(4)-Cd(3)-O(3)#4	96.62(14)
O(2)-Cd(2)-O(10)#2	142.86(13)	N(4)-Cd(3)-O(13)#4	131.42(14)
O(2)-Cd(2)-N(14)#3	101.54(15)	N(4)-Cd(3)-O1W	83.89(17)
O(4)-Cd(2)-O(3)	55.11(11)	O(13)#4-Cd(3)-O(3)#4	90.50(14)
O(4)-Cd(2)-O(9)#2	152.85(14)	O(13)#4-Cd(3)-O1W	78.40(18)
O(4)-Cd(2)-O(10) #2	99.29(13)	O(16)-Cd(3)-O(3)#4	93.46(13)
O(9)#2-Cd(2)-O(3)	113.78(12)	O(16)-Cd(3)-N(4)	134.54(16)
O(9)#2-Cd(2)-O(10) #2	55.56(13)	O(16)-Cd(3)-O(13)#4	92.53(16)
O(16)-Cd(3)-O1W	96.62(16)	Cd(3)#5-O(3)- Cd(2)	103.34(11)
[1]+X,-1+Y,+Z; [2]+X,1+Y,+Z; [3]2-X,2-Y,-Z; [4]+X,+Y,-1+Z; [5]+X,+Y,1+Z; [6]1-X,-Y,4-Z; [7]-X,-Y,4-Z			

Table S3 Comparison of gas adsorption properties and other reported MOFs.

MOF	CO_2 (cm^3 g^{-1})		Ref
	273 K	298 K	
CUST-607	70.69	23.61	In this work
$\{[Zn_5(L1)(btz)_6(H_2O)$-$(NO_3)]\cdot 5DMA\cdot 5H_2O\}_\infty$	42.79	25.96	[S2]
$\{[Zn_9(L2)_2(btz)_{12}]\cdot 14H_2O\}_\infty$	46.23	29.12	[S2]
MOF-235	-	0.17 m mol g^{-1}	[S4]
$Cu(4,4'$-$bpy)_2(OTf)_2$	-	17.8	[S5]
MOF-205-OBn	17.5	9.5	[S6]
Mg-MOF-74-1	105.0	80.5	[S7]
Mg-MOF-74-2	153.6	114.3	[S7]
Mg-MOF-74-3	181.4	137.9	[S7]
$[Zn(btzip)(H_2O)_{0.5}]\cdot H_2O$	36.2	29.8	[S8]

Table S4 A comparison of K_{SV} for detecting TNP and other reported MOFs.

MOF	K_{SV}	Ref
$[Cd_3(H_2O)($ $H3L)_2(dia)_2]\cdot DMA\cdot 2H_2O$	1.43×10^5 M^{-1}	In this work
$[Cd(INA)(pytpy)(OH)\cdot 2H_2O]_n$	4.30×10^4 M^{-1}	[S9]
[Tb(L)(OH)]·x(solv)	7.73×10^{-2} ppm^{-1}	[S10]
AHU-TW6	5.31×10^4 M^{-1}	[S11]
Zr-NDC/Tz and Zr-NDC/CN)	1.8×10^4 M^{-1}	[S12]
$[Cd(NDC)_{0.5}(PCA)]$.xG	3.5×10^4 M^{-1}	[S3]
$[(CH_3)_2NH_2]_3[Zn_4Na(BP$ $TC)_3]\cdot 4CH_3OH\cdot 2DMF$	3.2×10^4 M^{-1}	[S13]
$[Zn(NDC)(H_2O)]_n$	6×10^4 M^{-1}	[S14]
$[Cd(NDC)(H_2O)]_n$	2.385×10^4 M^{-1}	[S14]
$\{[Tb(L)_{1.5}(H_2O)]\cdot 3H_2O\}_n$	7.47×10^4 M^{-1}	[S15]

Reference

[S1] C. H. Ke, H. M. Lee, Nickel coordination polymers with $\{4^8.6^2\}$ and bnn topologies constructed from common square-pyramidal 5-connected nodes, *CrystEngComm*, 2012, 14, 4157-4160.

[S2] Y. Q. Chen, Y. K. Qu, G. R. Li, Z. Z. Zhang, Z. Chang, T. L. Hu, J. Xu, X. H. Bu, Zn(II)-benzotriazolate clusters based amide functionalized porous coordination polymers with high CO_2 adsorption selectivity, *Inorg. Chem*, 2014, 53, 8842-8844.

[S3] S. S. Nagarkar, B. Joarder, A. K. Chaudhari, S. Mukherjee and S. K. Ghosh, Highly selective detection of nitro explosives by a luminescent metal-organic framework, *Angew. Chem., Int. Ed*, 2013, 52, 2881-2885.

[S4] M. Anbia, V. Hoseini, S. Sheykhi. Sorption of methane, hydrogen and carbon dioxide on metal-organic framework, iron terephthalate (MOF-235), *J Ind Eng Chem*, 2012, 18(3), 1149-1152.

[S5] X. Q. Wang, L. B. Li, J. F. Yang, J. P. Li. CO_2/CH_4 and CH_4/N_2 separation on isomeric metal organic frameworks, *Chinese J Chem Eng*, 2016, 24(12), 1687-1694.

[S6] J. Sim, H. Yim, N. Ko, S. B. Choi, Y. J. Oh, H. J. Park, S. Y. Park, J. Kim, Gas adsorption properties of highly porous metal–organic frameworks containing functionalized naphthalene dicarboxylate linkers, *Dalton Trans,* 2014, 43, 18017-18024.

[S7] Z. Y. Yao, J. H. Guo, P. Wang, Y. Liu, F. G, W. Y. Sun, Controlled synthesis of micro/nanoscale Mg-MOF-74 materials and their adsorption property, *Mater Lett*, 2018, 223, 174-177.

[S8] W. J. Shi, Y. Z. Li, Q. X. Hu, G. D. Wang, L. Hou, Y. Y. Wang, New scu topological MOF based on azolyl-carboxyl bifunctional linker: Gas adsorption and luminescence properties, *J Solid State Chem*, 2020, 283, 121170.

[S9] J. Zhang, J. Wu, G. Tang, J. Feng, F. Luo, B. Xu, C. Zhang, Multiresponsive water-stable luminescent Cd coordination polymer for detection of TNP and Cu^{2+}, *Sens. Actuators B*, 2018, 272, 166-174.

[S10] J. Qin, B. Ma, X. F. Liu, H. L. Lu, X. Y. Dong, S. Q. Zang, H. Hou, Aqueous- and vapor-phase detection of nitroaromatic explosives by a water-stable fluorescent microporous MOF directed by an ionic liquid, *J. Mater. Chem. A*, 2015, 3, 12690.

[S11] D. Wang, Z. Y. Hu, S. S Xu, D. D Li, Q. Zhang, W. Ma, H. P. Zhou, J. Y. Wu, Y. P. Tian, Fluorescent metal–organic frameworks based on mixed organic ligands: new candidates for highly sensitive detection of TNP, *Dalton Trans*, 2019, 48,1900.

[S12] M. Gutiérrez, R. Navarro, F. Sánchez, A. Douhal, Photodynamics of Zr-based MOFs: effect of explosive nitroaromatics, *Phys. Chem. Chem. Phys*, 2017, 19, 16337.

[S13] E. L. Zhou, P. Huang, C. Qin, K. Z. Shao and Z. M. Su, A stable luminescent anionic porous metal-organic framework for moderate adsorption of CO_2 and selective detection of nitro explosives, *J. Mater. Chem. A*, 2015, 3, 7224.

[S14] P. Ghosh, S. K. Saha, A. Roychowdhury, P. Banerjee, Recognition of an explosive and mutagenic water pollutant, 2,4,6-Trinitrophenol, by cost-effective luminescent MOFs, *Eur. J. Inorg. Chem*, 2015, 17, 2851-2857.

[S15] L. H. Cao, F. Shi, W. M. Zhang, S. Q. Zang and T. C. W. Mak, Selective sensing of Fe^{3+} and Al^{3+} ions and detection of 2,4,6-Trinitrophenol by a water-stable terbium-based metal-organic framework, *Chem. Eur. J*, 2015, 21, 15705.